ELSEVIER

Journal of Molecular Catalysis A: Chemical 131 (1998) 91–106

JOURNAL OF MOLECULAR CATALYSIS A: CHEMICAL

The surface and catalytic chemistry of olefin metathesis catalyzed by metallic and oxygen-modified molybdenum

Gefei Wu, Brian Bartlett, Wilfred T. Tysoe *

Department of Chemistry and Laboratory for Surface Studies, University of Wisconsin-Milwaukee, Milwaukee, WI, USA

Received 5 May 1997; revised 30 July 1997; accepted 4 August 1997

Abstract

It is shown that model oxides grown on metallic substrates catalyze propylene metathesis to form ethylene and butene with an activity that mimics that of supported catalysts for reaction below ~650 K. Another regime is found above ~650 K where the reaction proceeds with a much higher activation energy of ~60 kcal/mol. Unfortunately, alkenes do not react to any detectable extent on the model oxide surfaces in ultrahigh vacuum. However, the high-temperature (>650 K) metathesis rate is found to be effected by the presence of oxygen overlayers, which also modify the chemistry of alkenes on Mo(100) in ultrahigh vacuum. Methane is formed in temperature-programmed desorption following adsorption of alkenes (ethylene, propylene and 2-butene) on O/Mo(100). The only other products detected are ascribed to either hydrogenation reactions or to total thermal decomposition into carbon and hydrogen and it is proposed that alkenes dissociate via C=C bond cleavage forming carbenes which then hydrogenate to yield methane. This chemistry is in accord with that found catalytically at high temperatures where the product distribution from the reaction of ethylene is well described by a Schulz–Florey distribution and the product distribution from propylene is well described by co-polymerization of carbenes and methyl carbenes. The reaction is also found to proceed in the presence of a carbonaceous layer which appears to consist of both adsorbed hydrocarbons and graphite. The adsorbed hydrocarbons are removed by hydrogen with fairly low activation energy (~6.5 kcal/mol) and it is also shown that the rate of olefin metathesis is accelerated by the addition of hydrogen to the reaction mixture. Since this reaction does not require hydrogen to proceed, this effect is ascribed to a removal of these strongly bound hydrocarbons which increases the number of reactions sites on the surface.

Keywords: Methane; Metathesis; Carbenes

1. Introduction

The randomization of alkylene groups in alkenes, that is, their metathesis, is essentially thermoneutral since the number and type of carbon–carbon bonds are conserved for reactants and products. The reaction was discovered in 1931 where it was demonstrated by Schneider and Frölich [1] that heating propylene to high temperatures indeed formed the thermodynamically predicted products. The rate is limited by the high activation energy for the reaction and is a classical example of a Woodward–Hoffmann (electronic symmetry) forbidden reaction [2]. A heterogeneous catalyst for the reaction was discovered over 30 years later by Banks and Bailey [3] who found that alumina-

* Corresponding author. Tel.: +1-414-229-5222; fax: +1-414-229-5036; e-mail: wtt@csd.uwm.edu

1381-1169/98/$19.00
PII S1381-1169(97)00258-6

supported molybdena catalyzed the metathesis of propylene to ethylene and butene with rather high selectivity below ~ 650 K with an activation energy of ~ 6 kcal/mol [4,5], substantially lower than the value in the absence of a catalyst. Early theories for the effectiveness of the metathesis catalyst were framed in terms of lowering the activation barrier of a surface C_4 intermediate transition state [6–8] by having the substrate orbitals participate in bonding to the reaction transition state and thereby acting as an electron sink to lower the transition state energy. This situation has been discussed in detail in a classical paper by Schachtschneider [9]. However, work with homogeneous catalysts lead to the proposal of an alternative, two-step model which suggested that reaction was initiated by the formation of a carbene. In homogeneous phase, this is often provided by including a co-catalyst. The carbene is then proposed to constitute the active catalytic site by reacting with an alkene to produce a metallocyclic intermediate [10–19] [20–26]. This can potentially react via several routes, for example, by reductive elimination to yield cyclopropane [27] or a hydrogen transfer produces an alkene [28]. Both of these reactions, of course, destroy the initial carbene active site. Finally, the metallacycle can react via the reverse of its formation pathway to yield an alkene and reform a surface carbene resulting in an overall metathesis reaction since a carbon–carbon double bond has effectively been broken and remade [10–26]. In fact, in this pathway, complete scission of the double bond is not required (except for the initial carbene synthesis), presumably resulting in a lowering of the reaction activation energy. The carbene can also be consumed by reacting with other carbenes analogously to the polymerization step in Fischer–Tropsch synthesis [29]. This, of course, also effectively constitutes olefin metathesis since carbon–carbon bonds are cleaved and reassembled.

It is also found that the activity of the molybdenum (and also tungsten and rhenium) catalysts depend on the oxidation state of the metal [30,31] so that supported metallic (M(0)) catalysts are considered to be completely inactive and some higher oxidation state, often thought to be $+4$, is the most active for the reaction. In the following, the nature of the most active catalyst and possible pathways for the reaction are probed using surface science and catalytic strategies on well-characterized model samples.

2. Experimental

Experiments were performed using a range of pieces of apparatus, all of which have been discussed in detail elsewhere [32,33]. Temperature-programmed desorption data were collected using a bakeable, stainless-steel chamber operating at a base pressure of $\sim 5 \times 10^{-11}$ Torr which was equipped with capabilities for multimass, temperature-programmed desorption, low-energy electron diffraction and Auger spectroscopy. The sample could be heated to ~ 2100 K using electron-beam heating and cooled to ~ 80 K by thermal contact with a liquid-nitrogen-filled reservoir.

Catalytic reactions were carried in a chamber evacuated by means of a diffusion pump which operated at base pressure of 1×10^{-10} Torr [34]. This chamber also incorporated a co-axial, high-pressure reactor which could be pressurized to ~ 800 Torr while maintaining ultrahigh vacuum in the rest of the apparatus. The gas was recirculated within the cell by means of a gas pump and the reaction rate was determined by measuring the gas composition periodically by diverting a small portion of the reactant mixture to a gas chromatograph for analysis. Reaction rates are calculated directly from a product accumulation curve for low ($< 1\%$) conversions. This sample could also be heated to ~ 2000 K and cooled by contact with a liquid-nitrogen-chilled reservoir.

Ultraviolet photoelectron spectra were obtained at the Wisconsin Synchrotron Radiation Center using the Aladdin storage ring [35]. The stainless-steel, ultrahigh vacuum chamber used

for these experiments operated at a base pressure of $\sim 1 \times 10^{-10}$ Torr following bakeout and was attached to the end of a Mark V Grasshopper monochromator. The chamber was equipped with a quadrupole mass analyzer for residual gas analysis and to test gas purities. It was also equipped with a double-pass, cylindrical-mirror analyzer which was used to collect both Auger and photoelectron spectra.

The sample was cleaned by heating in $\sim 2.5 \times 10^{-7}$ Torr of oxygen at 1200 K for 5 min to remove carbon and then rapidly heated in vacuo to 2100 K to remove oxygen. This resulted in the diffusion of further carbon to the surface and this procedure was repeated until no impurities, particularly carbon, were noted on the surface after heating to 2100 K.

Oxygen overlayers were prepared by saturating the Mo(100) surface (20 L O_2 exposure at 1050 K; 1 L $= 1 \times 10^{-6}$ Torr s) and annealing to various temperatures to remove oxygen to obtain the requisite coverage. The adsorption of oxygen on Mo(100) has been studied very extensively [36–39] and the oxygen coverages were reproduced from their characteristic LEED patterns and confirmed from their relative O/Mo Auger ratios (by monitoring the O KLL and Mo LMM Auger transitions). MoO_2 films were grown using a literature protocol [40], which provides a surface that is active for olefin metathesis, where metallic molybdenum was oxidized using 3×10^{-5} Torr of oxygen for 120 s with the sample heated to 1050 K [41].

Alkenes were transferred to glass bottles and further purified by repeated bulb-to-bulb distillations and stored in glass until use. The oxygen (AGA Gas, 99%) was transferred from the cylinder to a glass bulb and also redistilled.

3. Results

3.1. Catalytic activity of model oxides

The metathesis activity of various model molybdenum oxide catalysts was tested in the high-pressure reactor using 450 Torr of propylene at a catalyst temperature of 650 K, and the results are displayed in Fig. 1 in histogram form. The errors in the measured rates are $\pm 10\%$. Metallic molybdenum is inactive under these reaction conditions and both MoO_2 and MoO_3 films catalyze olefin metathesis. Shown for comparison is the activity of a supported molybdenum oxide catalysts with a relatively high catalyst loading (18.6%) [42] where the agreement between the activity of the model catalysts and the high-surface-area sample is good. The temperature dependence of the metathesis rate is shown plotted in Arrhenius form (ln(Rate) vs. $1/T$) in Fig. 2 and indicate that there are two distinct metathesis pathways. One predominates below ~ 650 K where the reaction activation energy is ~ 6 kcal/mol (a value similar to that found for heterogeneous metathesis catalysts [4,5]). Note also that the absolute rate for this model is similar to that for high-surface-area metathesis catalysts (Fig. 1) so that oxide films provide realistic models for the supported catalyst. Above 650 K, the reaction is dominated by a high-activation-energy

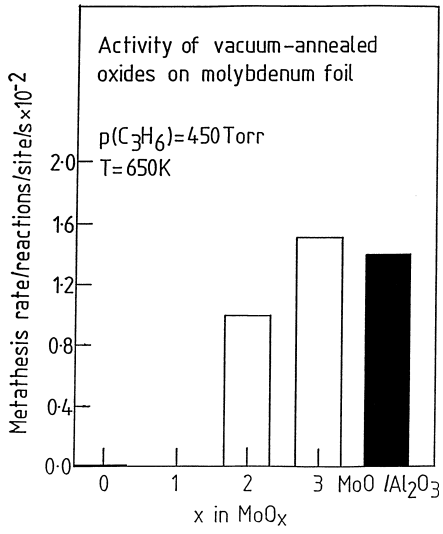

Fig. 1. Relative activity of various model molybdenum oxides for olefin metathesis using 450 Torr of propylene for reaction at ~650 K. Shown for comparison is the reactivity of a supported molybdenum oxide where the molybdenum loading is relatively high (18.6% [42]).

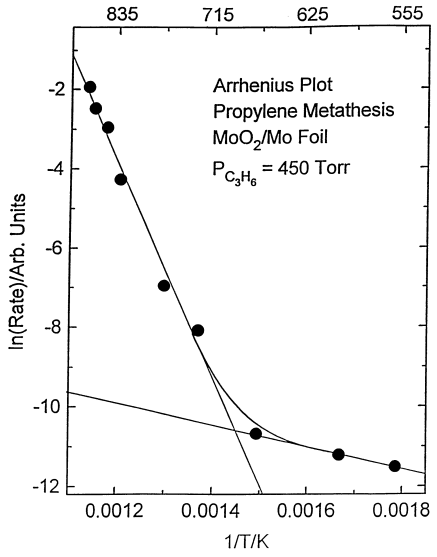

Fig. 2. Arrhenius plot for propylene metathesis catalyzed by MoO_2 using 450 Torr of propylene showing the two distinct reaction regimes.

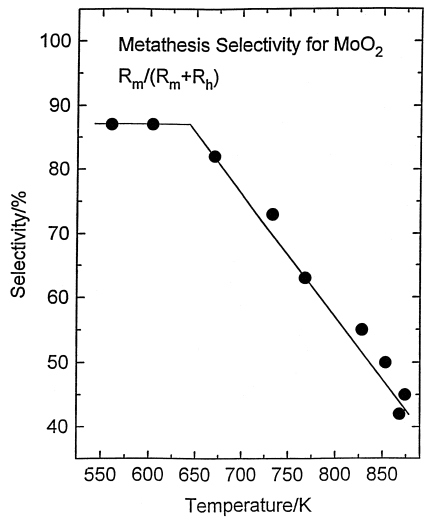

Fig. 3. Selectivity for olefin metathesis catalyzed by MoO_2 plotted as a function of temperature using 450 Torr of propylene again showing two different reaction regimes.

($E_{act} \sim 60$ kcal/mol) pathway. It is proposed that both of these routes operate simultaneously but the vast differences in their activation energies (and also correspondingly in their pre-exponential factors) means that they each dominate in different temperature regimes. Further evidence for different reaction pathways above and below 650 K come from the plot of metathesis selectivity plotted as a function of reaction temperature displayed in Fig. 3. In this case, the selectivity is rather high and constant below 650 K but decreases linearly with increasing reaction temperature above $\sim$650 K.

These results suggest that an MoO_2 film grown onto a polycrystalline molybdenum substrate appears to provide a reasonable model for a supported catalyst and therefore its surface chemistry is investigated further. Shown in Fig. 4 are a series of temperature-programmed desorption data collected in ultrahigh vacuum following ethylene adsorption (5 L) at 80 K on MoO_2. Unfortunately these results indicate that ethylene merely adsorbs molecularly on MoO_2 and desorbs intact at $\sim$190 K. The sharp peak at $\sim$100 K is due to a small amount of multilayer adsorption. Similar results are found for other alkenes, for example, propylene [43] and butene [44], adsorbed on MoO_2 indicating that this is an extremely unreactive surface in ultrahigh vacuum, in spite of being an active catalyst under higher-pressure conditions.

Fortunately, however, oxygen chemisorbed on Mo(100) effects its metathesis activity. This

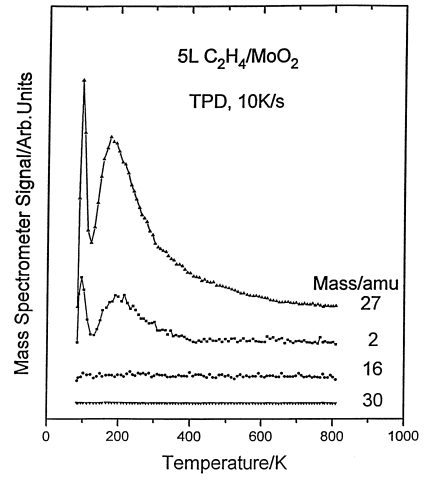

Fig. 4. Temperature-programmed desorption spectra collected following exposure of MoO_2 to 5 l of ethylene detecting 2, 16, 27 and 30 amu.

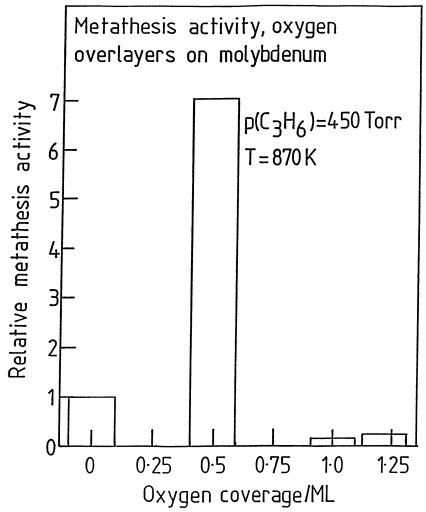

Fig. 5. The relative propylene metathesis activity of various oxygen overlayers on molybdenum at a catalyst temperature of 870 K (in the high-temperature regime) using 450 Torr of propylene.

is illustrated by the data in Fig. 5 which displays the relative metathesis activity in the high-temperature (and high-activation-energy) regime (above $\sim$650 K), using 450 Torr of propylene at 870 K. Again, errors in the measured catalytic rates are $\pm$10%. Under these conditions, metathesis is catalyzed by metallic molybdenum. The reactivity is, however, enhanced by the addition of oxygen to the surface where the presence of about 0.5 monolayers leads to a substantial rate increase, and coverages larger than one monolayer effectively poison the reaction. The chemistry of alkenes is therefore investigated on molybdenum surfaces modified by various overlayers of oxygen. As noted above, these can be prepared relatively easily [36–39] and also, as will be demonstrated below, exhibit a rich variety of chemistry as a function of oxygen coverage.

3.2. Surface chemistry of alkenes on oxygen-modified Mo(100)

It has been demonstrated previously that the binding energies of the 2s-derived molecular orbitals of a range of gas-phase hydrocarbons can be calculated rather accurately using Hückel theory [45,46]; that is, by taking the overlap integral S to be zero. This effect is illustrated in Fig. 6 which displays the photoelectron spectra due to the emission from 2s-derived molecular orbitals of several hydrocarbons adsorbed at 80 K on molybdenum [47]. Note that these electrons have relatively large binding energies (between 10 and 25 eV) and so may be described as shallow core levels. The peak positions are exactly what would be expected on the basis of simple molecular orbital calculations. This shallow core level spectroscopy is therefore sensitive to chemical changes at the surface, for example, to bond scission reactions, etc. This effect is further illustrated by the spectra of Fig. 7 which display the 2s region for ethylene adsorbed on metallic molybdenum at 80 K and heated to various temperatures. Two peaks are evident following adsorption at 80 K (also apparent in Fig. 6) indicating that ethylene adsorbs molecularly on molybdenum at this tempera-

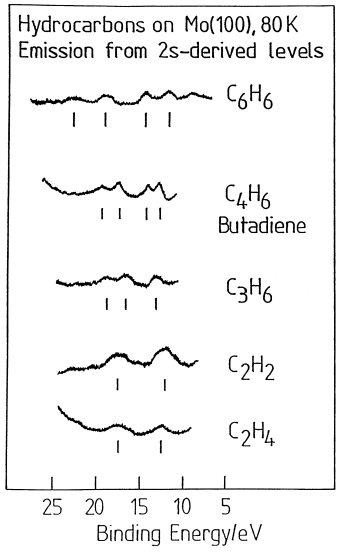

Fig. 6. Ultraviolet photoelectron spectra of various hydrocarbons adsorbed on Mo(100) at low temperature ($\sim$80 K) collected using 60 eV photons showing the 2s-derived molecular orbital region of the spectrum.

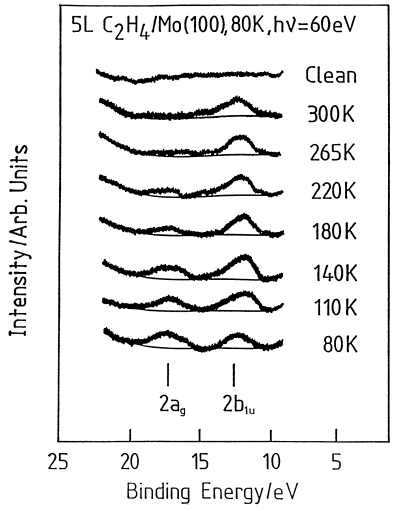

Fig. 7. The ultraviolet photoelectron spectra obtained following exposure of Mo(100) to 5 L of ethylene at 80 K and after heating to various temperatures. Spectra were collected using 60 eV photons and display only the 2s-derived region of the spectrum.

ture. The peaks are assigned to $2a_g$ and $2b_{1u}$ bonding and anti-bonding features, respectively as indicated on the figure. On heating, the higher-binding-energy feature decreases in intensity so that, by $\sim$265 K, the spectrum consists of a single peak at $\sim$12.5 eV binding energy suggesting the formation of a surface C_1 species. These results imply that molybdenum facilitates carbon–carbon double bond cleavage. This chemistry is in complete contrast to that found on group VIII metals where carbon–carbon bonds remain intact up to relatively high temperatures but is consistent with the first step in the carbene/metallocycle metathesis mechanism [10–26].

Further evidence for ethylene dissociation is presented in Fig. 8 which shows the 16 amu (methane) desorption spectra collected following adsorption of ethylene at 80 K on oxygen-modified Mo(100), where oxygen coverages are marked adjacent to the corresponding spectrum. Methane is detected, although metallic molybdenum, in spite of photoelectron spectroscopic evidence that C_1 species are formed (Fig. 7), desorbs no methane. However, methane is formed following ethylene adsorption on oxygen-covered surfaces where the maximum yield is found from a surface covered with 0.67 monolayers of oxygen (Fig. 8) confirming dissociative adsorption of ethylene. In order to test whether methylene hydrogenation is feasible on molybdenum, methylene species were grafted onto the surface by exposing it to methylene iodide. The resulting temperature-programmed desorption spectra are shown in Fig. 9. A relatively small amount of methane is formed in the absence of co-adsorbed hydrogen. However, predosing the Mo(100) sample with only 0.01 L of hydrogen results in a substantial enhancement in the rate of methane formation. Higher hydrogen exposures lead to further, although less dramatic, increases in methane yield. Thus, adsorbed methylene species can react with surface hydrogen to form methane [48]. The methane desorption temperature found following methylene iodide adsorption (Fig. 9) is substantially lower than following ethylene adsorp-

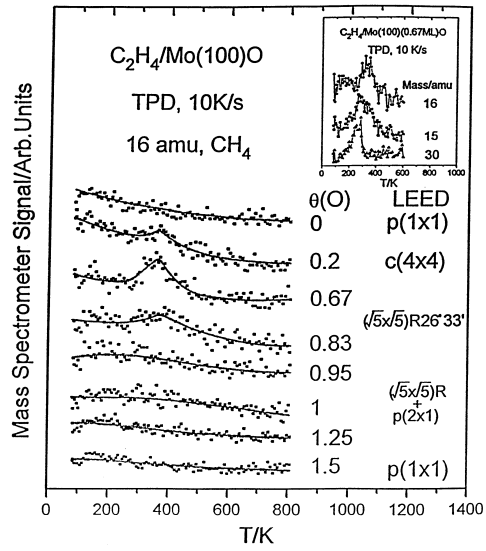

Fig. 8. Sixteen atomic mass units (CH_4) temperature-programmed desorption spectra collected following adsorption of ethylene on various oxygen-covered Mo(100) surfaces. The oxygen coverages are displayed adjacent to the corresponding spectra. Shown as an inset are the 16, 15 and 30 amu spectra obtained following adsorption of ethylene on a Mo(100) surface covered by 0.67 monolayers of oxygen.

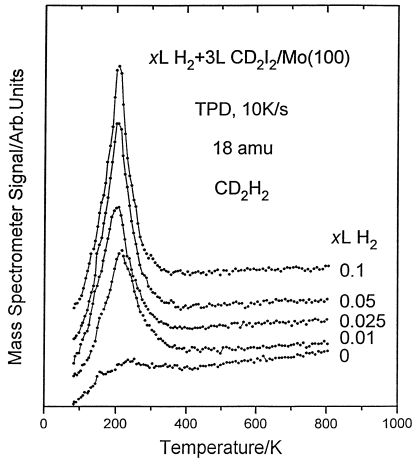

Fig. 9. Eighteen atomic mass units (CH_2D_2) thermal desorption spectra collected by adsorbing methylene iodide on Mo(100) with various hydrogen pre-coverages. The hydrogen dose is displayed adjacent to each spectrum.

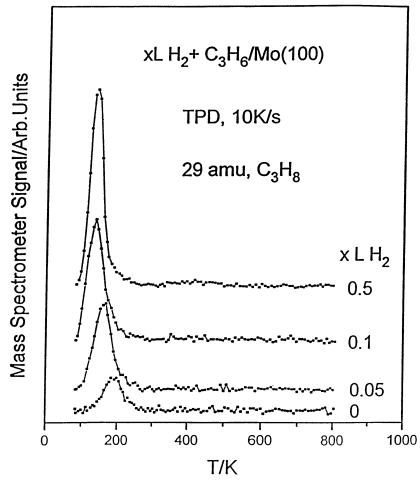

Fig. 10. Twenty nine atomic mass units (propane) temperature-programmed desorption spectra obtained by adsorbing propylene on a hydrogen pre-covered surface as a function of hydrogen exposure. Hydrogen exposures are marked adjacent to each spectrum.

tion (Fig. 8) ($\sim$ 220 K vs. $\sim$ 380 K). The origin of this difference is not known but is likely associated with the effect of the relatively large iodine atom also present of the surface along with the hydrocarbon fragment which may have the effect of forcing the species onto another adsorption site [49].

Note that no ethylene was formed by coupling of methylene species on the surface either after dosing methylene iodide or by monitoring possible isotope scrambling products after dosing the surface with $^{13}C^{12}CH_4$. The only other reaction pathways found for ethylene on molybdenum were self-hydrogenation and thermal decomposition to yield carbon and hydrogen.

The chemistry of other unsaturated hydrocarbons was examined on various oxygen-pre-covered surfaces in order to establish whether similar reactivity patterns are found in these cases. Fig. 10 displays the 29 amu (propane) desorption spectra obtained by adsorbing propylene onto a hydrogen-pre-covered Mo(100) surface as a function of hydrogen exposure. Clearly, molybdenum catalyzes alkene hydrogenation and this catalytic reaction has been investigated at higher pressures [50]. The clear decrease in peak temperature as the hydrogen coverage increases indicates a second-order reaction with surface hydrogen. Note again the large increase in hydrogenation product yield with the addition of relatively small amounts of hydrogen. Fig. 11 displays the corresponding methane desorption spectra from propylene adsorbed on various oxygen-covered Mo(100) surfaces. Once again, methane is synthesized but with overall yields

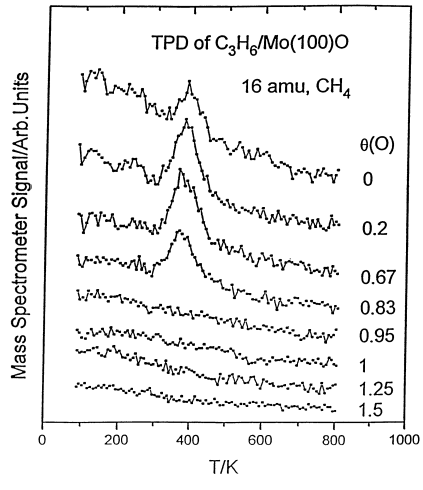

Fig. 11. Sixteen atomic mass units (methane) temperature-programmed desorption spectra collected after exposing various oxygen pre-covered surfaces to propylene. The oxygen coverages are marked adjacent to each spectrum.

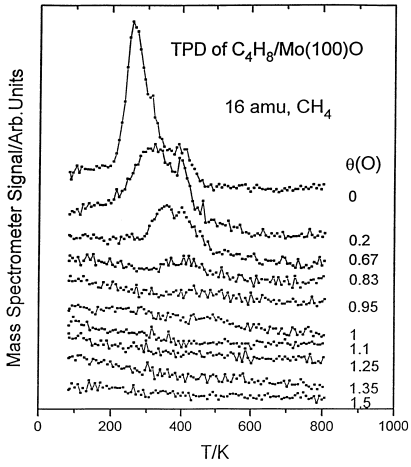

Fig. 12. Sixteen atomic mass units (methane) temperature-programmed desorption spectra collected after exposing various oxygen pre-covered surfaces to 2-butene. The oxygen coverages are marked adjacent to each spectrum.

larger than those found for ethylene adsorbed on these surfaces (Fig. 8). Methane desorbs from metallic molybdenum following adsorption of propylene and the yield increases with increasing oxygen coverage up to a maximum for an oxygen coverage of 0.67 and decreases at higher coverages. Note that the methane desorption peak temperature is 400 K, essentially identical to that found following ethylene adsorption (Fig. 8) but, as noted above, higher than that found following methylene iodide adsorption (Fig. 9). In addition, no ethylene or ethane desorption was detected following the adsorption of propylene on any oxygen-covered Mo(100) surfaces. However, hydrogen desorbs from the surface due to the thermal decomposition of propylene.

The corresponding methane desorption data obtained following 2-butene adsorption on Mo(100) are displayed in Fig. 12 where again substantial amounts of methane are formed. Now the peak temperature varies with oxygen coverage so that, on metallic molybdenum, methane desorbs at $\sim$260 K, close to the temperature found for methane formation after dosing either methylene iodide or methyl iodide on these surfaces with a shoulder at 400 K, closer to the methane desorption temperature after ethylene or propylene adsorption (Figs. 8 and 11). The low-temperature feature shifts to higher temperatures with increasing oxygen coverage and the 400 K peak remains essentially unaffected. The yield decreases with increasing oxygen coverage although the amount of methane formed is considerably larger than for both ethylene and propylene adsorption. The only other reaction pathways noted for 2-butene adsorbed on clean and oxygen-modified Mo(100) were hydrogenation to butene and complete dehydrogenation to carbon and hydrogen. No other C_3 or C_2 hydrocarbons were detected.

In order to further probe possible reaction pathways for 2-butene on Mo(100), photoelectron spectra were collected using 60 eV photons as a function of annealing temperature. The results are displayed in Fig. 13. The traces are obtained by subtracting the spectrum of clean Mo(100) from those of adsorbate-covered surfaces in order to accentuate the adsorbate-induced features. Particularly emphasized are the 2s-derived orbitals. The experimental positions for a condensed 2-butene layer (formed at 80 K)

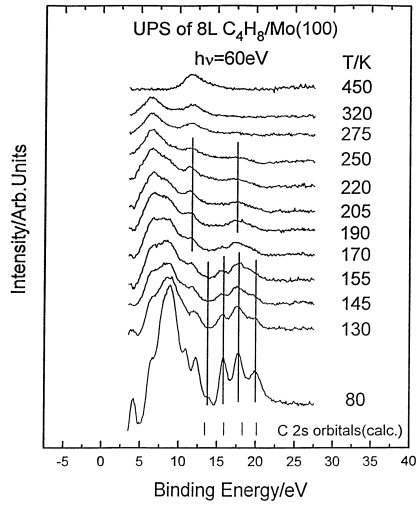

Fig. 13. Ultraviolet photoelectron spectra collected using 60 eV photons following adsorption of 2-butene on Mo(100) as a function of annealing temperature. Annealing temperatures are marked adjacent to each spectrum. Also indicated are the positions of peaks calculated for the 2s-derived molecular orbitals of 2-butene and the corresponding positions for a C_2 hydrocarbon.

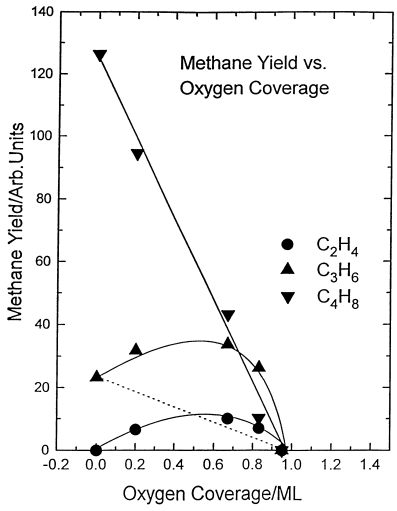

Fig. 14. Plot of the methane yield vs. oxygen coverage for ethylene (●), propylene (▲) and 2-butene (▼) on oxygen-covered Mo(100).

are compared with binding energies calculated for 2-butene from Hückel theory using the prescription outlined by Potts and Streets [45] and Streets and Potts [46]. The multilayer desorbs on heating the sample to ~130 K resulting in a significant attenuation in intensity. Nevertheless, the position of the peaks, in particular those in the 2s region, are identical to those for the molecular overlayer indicating that 2-butene adsorbs intact at this temperature, in accord with the temperature-programmed desorption results showing that hydrogenation products are formed. The peak positions remain essentially unchanged up to ~155 K. However, the features evolve into two peaks on heating to ~190 K indicating the formation of a C_2 hydrocarbon. Further heating to 275 K results in the appearance of only a single peak at a binding energy of 12.5 eV consistent with the detection of methane in temperature-programmed desorption (Fig. 12). It is important to note that there is no evidence for the intervention of any other C_4 or C_3 species that precede the formation of an adsorbed C_2 hydrocarbon. This implies that the carbon–carbon double bond dissociates forming two methyl carbenes in a reaction analogous to that seen above for ethylene. These are identified as the C_2 hydrocarbons detected by photoelectron spectroscopy between 190 and 250 K (Fig. 13).

Finally, shown plotted in Fig. 14 is the methane yield for ethylene, propylene and 2-butene adsorbed on various oxygen-covered surfaces. Note that the total methane yield increases with increasing carbon number so that 2-butene evolves substantially more methane than either ethylene or propylene. However, the methane yield from ethylene is a maximum for an oxygen coverage of ~0.6 and is zero for $\theta_O = 0$ and 1.0. The methane yield from 2-butene decreases linearly with increasing oxygen coverage and the yield from propylene is essentially a linear combination of the two effects. This can be understood in terms of the proposed carbene formation chemistry. CH_2 species are formed from ethylene where the resulting methane yield is the largest for a surface covered by 0.6 monolayers of oxygen. 2-Butene forms only methyl carbenes which thermally decompose to yield methane and, in this case, the methane yield decreases linearly with increasing oxygen coverage. Propylene dissociates to form equimolar amounts of meth-

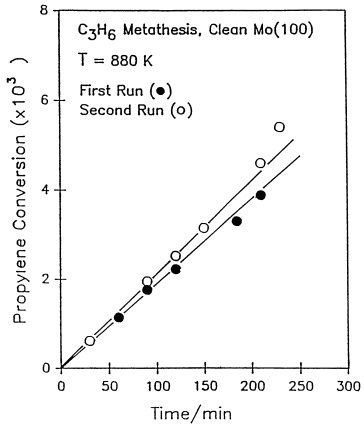

Fig. 15. Restart reaction for olefin metathesis catalyzed by metallic molybdenum at 880 K showing the product accumulation curve for an initially clean Mo(100) sample (●) and after removing this sample into ultrahigh vacuum and restarting the reaction with fresh propylene without cleaning the sample (○).

ylidenes and ethylidenes so that the variation in methane yield with oxygen coverage is this case is merely a linear combination of the yields of methane from ethylene and 2-butene as found experimentally (Fig. 14).

3.3. Nature of the catalyst surface and the effect of hydrogen

Analysis of the surface of either metallic molybdenum or molybdenum oxides after reac-

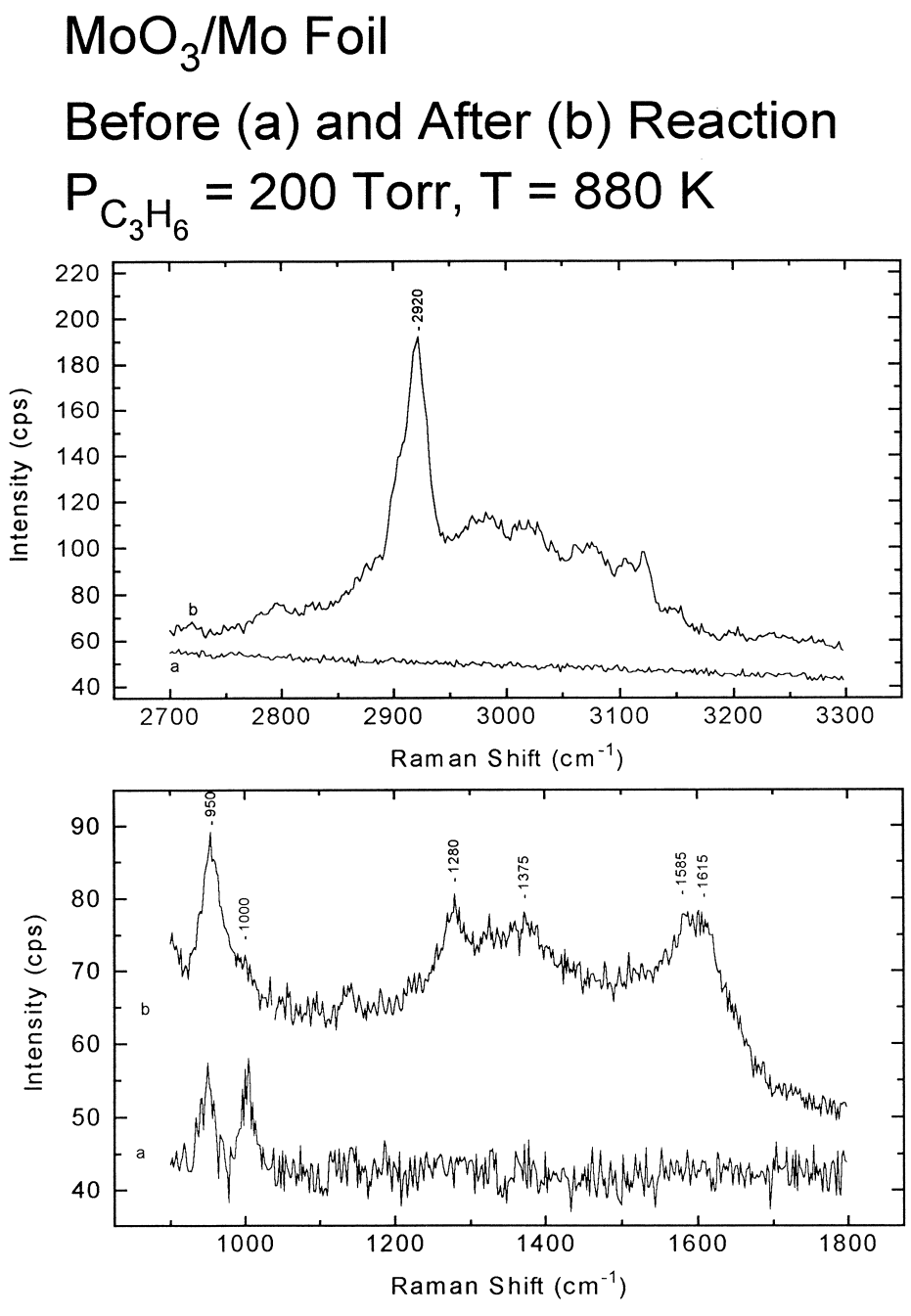

Fig. 16. Raman spectrum of an MoO_3 model catalysts before (a) and after (b) reaction with 200 Torr of propylene at 880 K.

tion using Auger spectroscopy reveals the presence of substantial amount of carbon. An estimate of the film thickness, using standard electron escape depths, suggests that the layer is the equivalent of several monolayers of carbon thick. In order to test whether the presence of this layer affects the catalytic activity, a 'restart' reaction was carried out and the results are displayed in Fig. 15. A metathesis product accumulation curve for catalysis by an atomically clean Mo(100) single crystal is shown. The sample is then removed into ultrahigh vacuum and the presence of large amounts of carbon confirmed using Auger spectroscopy. The sample is then reinserted into the high pressure cell which is filled to the same pressure of propylene as the first reaction and the reaction restarted over the carbon-covered sample. The product accumulation curve for this reaction is essentially identical to the rate on the initially clean surface indicating that olefin metathesis apparently takes place in the presence of this thick carbon layer. Similar restart experiments have been carried out on model oxide catalysts with identical results [51].

The nature of this layer can be probed on an

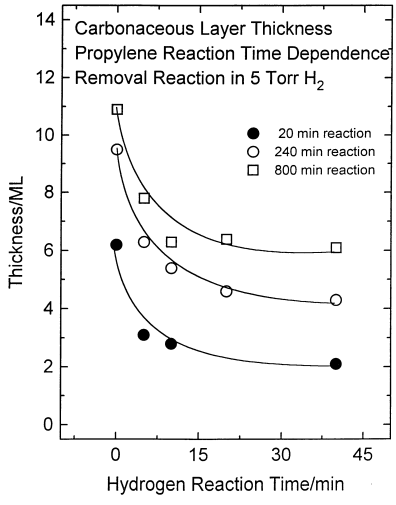

Fig. 17. Plot of layer thickness measured using Auger spectroscopy of the carbon films formed after reaction in propylene (450 Torr, 880 K) plotted as a function of reaction time in 5 Torr of hydrogen at 600 K after various times of reaction; (●) 20 min, (○) 240 min and (□) 800 min.

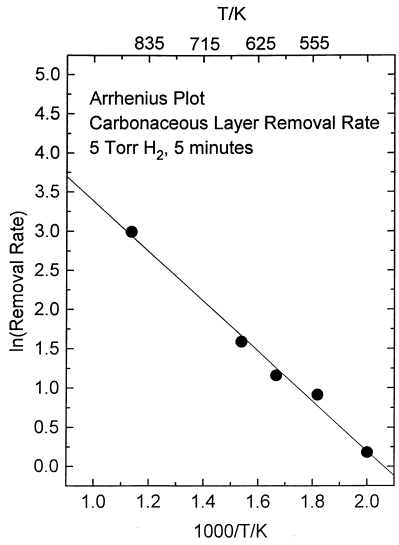

Fig. 18. Arrhenius plot for the removal by reaction with 5 Torr hydrogen of the hydrocarbon layer formed on molybdenum following reaction in propylene (450 Torr, 880 K).

MoO_3 substrate using Raman spectroscopy and the results are displayed in Fig. 16. This exhibits features between 2900 and 3100 cm^{-1} due to C–H stretching modes indicating that a substantial proportion of the carbon is present as a hydrocarbon. Also indicated are broad features with peaks at $\sim$1375 and 1600 cm^{-1} which have been assigned to the presence of graphitic species and so indicates that a portion of the carbon present on the surface is graphitic [52,53]. The graphitic carbon is not likely to react with hydrogen. However, as shown in Fig. 17, a portion of the carbon can be removed from the surface by reaction in 5 Torr of hydrogen at 600 K where part of the carbon is removed in $\sim$20 to 25 min irrespective of the time for which the carbon was deposited during olefin metathesis. There is, however, a portion of the carbon that apparently cannot be removed by reaction with hydrogen and the amount of this carbon increases with reaction time. The carbon that can be removed with hydrogen is associated with the hydrocarbon species evident in the Raman spectra of Fig. 16 and the part that cannot be removed is likely to be due to the graphitic species also detected by Raman spec-

troscopy. The temperature dependence of the hydrocarbon removal rate in the presence of 5 Torr of hydrogen is plotted in Arrhenius form in Fig. 18 which yields a relatively low value of hydrogenation activation energy of 6.4 ± 0.4 kcal/mol.

Since hydrogen can effectively remove carbon from the surface, and this carbon is likely to prevent access of reactants to the surface, it is postulated that addition of hydrogen will increase reactant accessibility to the surface and may result in an increase in reaction rate. The results of these experiments are shown in Fig. 19 which plots the rate of propylene metathesis (450 Torr, 800 K) vs. the pressure of hydrogen added to the mixture. It should be emphasized that hydrogenation and hydrogenolysis products are also formed which might be expected to lead to a decrease in the rate of olefin metathesis since reactants are being titrated from the surface whereas the data of Fig. 19 clearly show a rate enhancement in accord with the above postulate. The associated carbon film thickness found using Auger spectroscopy measured following reaction in the presence of hydrogen

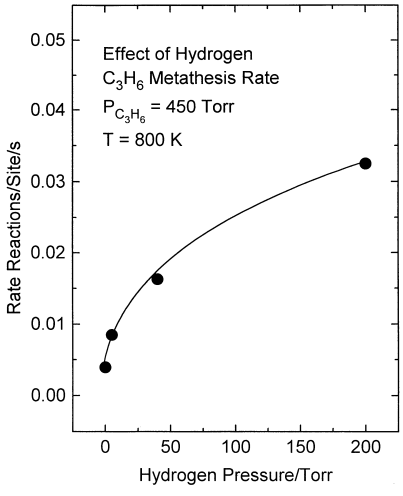

Fig. 19. Plot showing the effect of addition hydrogen on the rate of propylene metathesis (450 Torr, 800 K) catalyzed by molybdenum where the metathesis rate is plotted vs. hydrogen pressure.

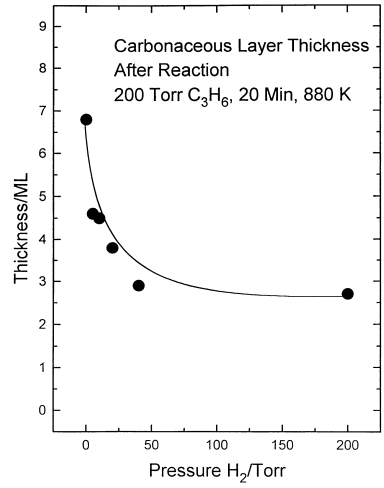

Fig. 20. Plot of the remaining carbonaceous layer thickness measured using Auger spectroscopy during propylene metathesis (200 Torr, 880 K) as a function of hydrogen pressure where the carbonaceous layer thickness is plotted vs. hydrogen pressure.

(Fig. 20) shows a clear decrease in the amount of carbon on the surface with increasing hydrogen pressure in accord with the suggestion made above.

4. Discussion

4.1. Synthesis of model catalysts, their surface properties and reaction pathway

Model olefin metathesis catalysts consisting of either MoO_2 or MoO_3 formed by oxidizing a molybdenum foil mimic the activity of supported metathesis catalysts for reaction below $\sim$ 650 K (Fig. 1). This reaction is also catalyzed in homogeneous phase and here reaction is suggested to be initiated by the formation of a carbene which is then proposed to react to form a metallacycle. This subsequently thermally decomposes by the reverse of this route to yield metathesis products [10–36]. Simultaneously, there is a high-activation-energy reaction pathway ($E_{act} \sim 60$ kcal/mol; Fig. 2) that predominates at high temperatures. Unfortunately, these model oxide catalysts are rather inactive in ultrahigh vacuum so that alkenes merely adsorb

and desorb molecularly and essentially undergo no surface chemistry (Fig. 4).

Fortunately, oxygen overlayers on Mo(100) also effect the metathesis activity of the catalyst in the higher-temperature regime (Fig. 5) so that the chemistry of alkenes is studied on these surfaces. These turn out to exhibit a rather rich surface chemistry which displays significant variations in reactivity as a function of oxygen coverage. This is illustrated by the data of Figs. 7 and 8 which show that ethylene adsorbs dissociatively on oxygen-covered molybdenum surfaces to yield surface carbenes. Grafting methylene species onto the surface by thermally decomposing iodine-containing precursors reveals that carbenes can react with adsorbed hydrogen to form methane. It has been shown that methane forms at the same temperature in temperature-programmed desorption when either methylene or methyl species are grafted onto Mo(100) from iodine-containing precursors [49]. This implies that the final addition of hydrogen to an adsorbed methyl species is the rate-limiting step in the methane formation pathway. The activation energy for methane formation, in the absence of co-adsorbed iodine, as measured from a leading-edge plot yields an activation energy to methane formation of ~ 23 kcal/mol. Previous estimates of the heat of adsorption of carbenes have yielded values ~ 100 kcal/mol [33]. As noted above, hydrogenation of a methyl group is, in fact, rate limiting which allows the heat of adsorption of a methyl group to be estimated from:

$$E(\mathrm{CH_4}) \sim \Delta H_{(\mathrm{ads})}(\mathrm{CH_3}) + \Delta H_{(\mathrm{ads})}(H) - D(\mathrm{CH_3}\text{–H})$$

where $\Delta H_{(\mathrm{ads})}(H)$ is the heat of adsorption of hydrogen on Mo(100) (~ 60 kcal/mol [54]) and $D(\mathrm{CH_3}\text{–H})$ the strength of the $\mathrm{CH_3}$–H bond (104 kcal/mol [55]). Using the activation energy for the formation of methane measured above, this yields an approximate value for the heat of adsorption of a methyl group of ~ 69 kcal/mol. Since the hydrogenation of this to methane is the rate-limiting step, the activation energy of hydrogenation of a methylene to a methyl moiety will be less than this value, so that $\Delta H_{(\mathrm{ads})}(\mathrm{CH_2})$ is less than 128 kcal/mol but substantially greater than 69 kcal/mol.

Reacting ethylene over metallic molybdenum at high pressures at catalyst temperatures above ~ 650 K leads to a series of higher hydrocarbons with a distribution that is well described by a Schulz–Florey plot [29]. This suggests that the high-temperature metathesis reaction (Figs. 2 and 3) is due to alkene dissociation and recombination of the resulting carbene species on the metal surface. The high activation energy for this reaction (~ 60 kcal/mol [29]) then reflects the large heat of adsorption of carbene species and can be used to estimate its heat of adsorption ignoring any substrate relaxation effects [33]. This yields a value of ~ 120 kcal/mol in reasonable agreement with the range estimated above. Note that this is an 'active site' removal pathway for the carbene-metathesis mechanism which may operate at lower temperatures [10–26]. The large activation energy for this pathway means that these species are removed only slowly at lower temperatures. The product distribution from the reaction of propylene can similarly be rationalized by assuming co-polymerization of equimolar amounts of carbenes and methyl carbenes indicating a similar high-temperature metathesis mechanism for propylene as for ethylene [51].

It is clear, at least on these oxygen modified surfaces, that carbene formation is rather facile. We turn our attention now to examining the way in which these species might form. Note that both propylene and 2-butene chemisorbed on O/Mo(100) decompose to yield methane indicating that they ultimately form either methyl or methylene species, which then hydrogenate. They can also self-hydrogenate in ultra-high vacuum forming alkanes (see for example Fig. 10) or completely thermally decompose producing carbon and hydrogen. No other products are formed. It has been suggested that carbenes can form from alkenes containing alkyl

groups via an initial alkyl dehydrogenation [56,57]. Under this proposal, the methyl group of propylene would react to form an allylic species. Hydrogenation of the allylic species at the β position would lead to the formation of a metallacycle which would then thermally decompose to yield ethylene and deposit a carbene. Note, first, that no ethylene is detected following propylene adsorption. Second, preliminary results obtained by adsorbing $CH_2=CH-CH_2I$ to form the allylic species onto various oxygen-modified surfaces results in the desorption of only hydrogen [58]. Attempts to hydrogenate this species at the β position merely result in the formation of a small amount of propane. An alternative pathway proposes partial hydrogenation of adsorbed alkenes to yield alkyl species [59]. This reaction clearly takes place since alkenes react to form alkanes which must form via an intervening alkyl species. The alkyl species is then proposed to decompose via an α-hydride elimination. In fact, alkyl species grafted onto these surface by adsorbing ethyl iodide thermally decompose to form ethylene via β-hydride elimination as generally found on transition metal surfaces [58].

In addition as noted above, the ultraviolet photoelectron spectroscopic data of Fig. 14 indicate that 2-butene thermally decomposes directly to form C_2 species (proposed to be methyl carbenes) without the participation of any other surface C_4 species. Both of the mechanisms outlined above would involve the intervening formation of other C_4 species, the former pathway involving a methyl metallacycle, the latter a methyl ethyl carbene. The formation of either of these intermediates would lead to significant changes in the 2s-derived peak positions which are not detected.

Finally, it is clear that the total methane yield increases substantially through the homologous series, ethylene, propylene, 2-butene (Fig. 14). Since it is proposed above that methane forms via a direct carbon=carbon double bond dissociation reaction to form carbenes, the variation in total methane yield may be related to this dissociation probability. It has been suggested that, within the context of the Dewar–Chatt–Duncanson model, alkenes bond on Mo(100) primarily by donation of electrons from π orbitals to the metal rather than via back donation into vacant π^* orbitals [60,61]. That is, alkenes behave like π-donors on Mo(100). Corroborative evidence for this idea comes from the effect on oxygen on alkene desorption activation energies which increase with the addition of oxygen to the surface in accord with the above proposal [35,43]. It should be emphasized that alkenes are likely to bond synergistically via both donation and acceptance of π electrons, but that electron donation to the surface predominates. The relatively large number of vacant d-orbitals available to accept electrons in molybdenum in comparison with, for example, group VIII metals, may partially rationalize the bonding mode in this case. The position of the π orbital in alkenes is substantially affected by the presence of a methyl group so that the binding energy of the π orbitals in ethylene is 10.5 eV, 9.7 eV in propylene and 9.1 eV in 2-butene [62]. These shifts are fairly large and indicate that the π orbital should be rather closer to the Fermi level in 2-butene than in ethylene. This indicates that the extent of electron donation from the π orbitals to the substrate should be larger for 2-butene than for ethylene leading to a larger decrease in bond order and therefore an increased bond dissociation probability in the order 2-butene > propylene > ethylene, as found experimentally. It is clear that the large methane yield found for 2-butene adsorbed on Mo(100) is also associated with the appearance of an addition methane desorption features at ~ 280 K (Fig. 12). This peak is rather close to that found for methane formation from methylene iodide (Fig. 9). It has also recently been suggested that the lower desorption temperature measured when hydrocarbon species are formed from iodine-containing precursors, is due to site blocking by the relatively large iodine atom. Similar occupation of other sites when many more C_1 species are present on the surface may

account for the additional low-temperature feature evident in Fig. 12.

4.2. Nature of the catalyst surface during reaction

Analysis of surface of the model metathesis catalyst after reaction yields an Auger spectrum having a strong carbon signal. By using electron escape depths and calibrating the Auger signal for a carbon monolayer allows approximate carbon film thicknesses to be estimated [34] and reveals that the carbon film is the equivalent of several monolayers in thickness and the results of the restart experiment shown in Fig. 15 indicates that reaction takes place in the presence of this layer. As indicated by the Raman data displayed in Fig. 16, it consists both of hydrocarbon and graphitic components and the data of Figs. 17 and 18 indicate that the carbonaceous portion of the film can be removed using high pressures of hydrogen at ~ 600 K and that the activation energy of this reaction is ~ 6.5 kcal/mol. The graphitic part of the carbon does not react with hydrogen and the results of Fig. 17 suggest that the amount of graphite on the surface increase as a function of time on stream implying that the carbonaceous layer slowly converts to graphite as the reaction proceeds. It is also found that adding hydrogen to propylene increases the rate of olefin metathesis (Fig. 19) and this effect is ascribed to the removal of carbonaceous species from the surface to reveal more active catalyst sites below. Corroborative evidence for this idea comes form the data of Fig. 20 which show the corresponding carbon thickness after olefin metathesis in the presence of hydrogen as a function of hydrogen pressure, where the amount of surface carbon decreases as the reaction rate increases. As noted above, the olefin metathesis reaction pathway at these high temperatures does not involve hydrogen so that the increase in reaction rate is not associated with this effect. It appears that hydrocarbon reactions are generally enhanced in rate by the addition of hydrogen and this effect has also been seen in the palladium-catalyzed formation of benzene from acetylene [63], another hydrocarbon conversion reaction that does not involve hydrogen. It is therefore likely that this also happens for reactions that do involve hydrogen as one of the reactants, for example, in alkene and alkyne hydrogenation, both of which proceed in the presence of carbonaceous layers. The implications of this phenomenon are being explored.

5. Conclusion

Alkenes react on oxygen-covered Mo(100) either to form alkanes, or to completely thermally decompose to form carbon and hydrogen or to adsorb dissociatively to yield carbene species. Both model molybdenum oxides and oxygen-covered Mo(100) catalyze olefin metathesis where two reaction pathways are found, one that predominates at low temperatures (< 650 K) and has a relatively low activation energy and another that predominates at higher temperatures, which has a much higher activation energy of ~ 60 kcal/mol. The latter reaction is proposed to proceed by recombination of the carbene fragments which adsorb relatively strongly on Mo(100) with a heat of adsorption of ~ 120 kcal/mol. This accounts for the rather high activation energy for this reaction. Catalysis proceeds in the presence of a carbonaceous layer which consists of a hydrocarbon portion which can be titrated away using high pressures of hydrogen and a graphitic portion that is unreactive. The catalytic reaction is accelerated by the addition of hydrogen and this is explained by assuming that hydrogen removes hydrocarbons to reveal metal sites below.

Acknowledgements

We gratefully acknowledge support of this work by the U.S. Department of Energy, Divi-

sion of Chemical Sciences, Office of Basic Energy Sciences, under Grant No. DE-FG02-92ER14289. This work is based upon research conducted at the Synchrotron Radiation Center, Univ. of Wisconsin–Madison, which is supported by the NSF under Award No. DMR-95-31009.

References

[1] V. Schneider, P.K. Frölich, Ind. Eng. Chem. 23 (1931) 1045.
[2] R.B. Woodward, R. Hoffmann, The Conservation of Orbital Symmetry, Academic Press, New York, 1972.
[3] R.L. Banks, G.C. Bailey, Ind. Eng. Chem. Prod. Res. Dev. 94 (1965) 60.
[4] E. Ogata, Y. Kamiya, Chem. Lett. (1973) 603.
[5] C.P.C. Bradshaw, E.J. Howman, L. Turner, J. Catal. 7 (1967) 269.
[6] C.T. Adams, S.G. Brandenberger, J. Catal. 13 (1969) 360.
[7] D.L. Crain, J. Catal. 13 (1969) 110.
[8] J.C. Mol, J.A. Moulijn, C. Boelhouwer, J. Catal. 11 (1968) 87.
[9] F.D. Mango, J.H. Schachtschneider, J. Am. Chem. Soc. 91 (1969) 1030.
[10] J.L. Hérisson, Y. Chauvin, Makromol. Chem. 141 (1970) 161.
[11] J.P. Soufflet, D. Commercue, Y. Chauvin, C.R. Hebd. Séances Acad. Sci. Ser. C. 276 (1973) 169.
[12] R.J. Haines, G.J. Leigh, Chem. Soc. Rev. 4 (1975) 155.
[13] C.P. Casey, T.J. Burkhardt, J. Am. Chem. Soc. 96 (1974) 7808.
[14] E.O. Fischer, K.H. Dotz, Chem. Ber. 105 (1972) 3966.
[15] R.R. Schrock, J. Am. Chem. Soc. 96 (1974) 6976.
[16] R.R. Schrock, J. Am. Chem. Soc. 98 (1976) 5399.
[17] B.A. Dolgoplosk, Dokl. Chem. 216 (1974) 380.
[18] R.H. Grubbs, P.L. Burk, D.D. Carr, J. Am. Chem. Soc. 97 (1975) 3265.
[19] R.H. Grubbs, D.D. Carr, C. Hoppin, P.C. Burk, J. Am. Chem. Soc. 98 (1976) 3478.
[20] T.J. Katz, J. Rothschild, J. Am. Chem. Soc. 98 (1976) 2519.
[21] T.J. Katz, W.H. Hersch, Tet. Lett. (1977) 585.
[22] C.P. Casey, H.E. Tuinstra, M.C. Seaman, J. Am. Chem. Soc. 98 (1976) 608.
[23] F.N. Tebbe, G.W. Parshall, D.W. Ovenall, J. Am. Chem. Soc. 101 (1979) 5074.
[24] J. Wengorius, R.R. Schrock, M.R. Churchill, J.R. Mussert, W.J. Young, J. Am. Chem. Soc. 102 (1980) 4515.
[25] T.R. Howard, J.B. Lee, R.H. Grubbs, J. Am. Chem. Soc. 102 (1980) 6878.
[26] R.H. Grubbs, T.K. Brunck, J. Am. Chem. Soc. 94 (1972) 25.
[27] F.J. McQuillan, K.G. Powell, J. Chem. Soc., Dalton Trans. (1972) 2123.
[28] W.S. Millman, M. Crespin, A.L. Cirrillo, S. Abdo, W.K. Hall, J. Catal. 60 (1979) 404.
[29] B. Bartlett, W.T. Tysoe, Catal. Lett. 44 (1997) 37.
[30] R.L. Burwell, A.J. Brenner, J. Mol. Catal. 1 (1975) 77.
[31] R. Thomas, J.A. Moulijn, J. Mol. Catal. 15 (1982) 157.
[32] L.P. Wang, W.T. Tysoe, Surf. Sci. 230 (1990) 74.
[33] G. Wu, B. Bartlett, W.T. Tysoe, Surf. Sci. 373 (1997) 129.
[34] L. Wang, C. Soto, W.T. Tysoe, J. Catal. 143 (1993) 92.
[35] G. Wu, B. Bartlett, W.T. Tysoe, Surf. Sci. 383 (1997) 57.
[36] H.M. Kennett, A.E. Lee, Surf. Sci. 48 (1975) 606.
[37] E.I. Ko, K.J. Madix, Surf. Sci. 109 (1981) 221.
[38] E. Bauer, H. Hoppa, Surf. Sci. 88 (1979) 31.
[39] C. Zhang, M.A. Van Hove, G.A. Somorjai, Surf. Sci. 149 (1985) 326.
[40] H.M. Kennett, A.E. Lee, Surf. Sci. 48 (1975) 624.
[41] B. Bartlett, V.L. Schneerson, W.T. Tysoe, Catal. Lett. 3 (1995) 1.
[42] R. Thomas, J.A. Moulijn, J. Mol. Catal. 15 (1982) 157.
[43] G. Wu, W.T. Tysoe, Surf. Sci. 391 (1997) 134.
[44] G. Wu, W.T. Tysoe, Surf. Sci. in press.
[45] A.W. Potts, D.G. Streets, J. Chem. Soc. Faraday II 70 (1974) 875.
[46] D.G. Streets, A.W. Potts, J. Chem. Soc. Faraday II 70 (1974) 1505.
[47] L.P. Wang, R. Hinkelman, W.T. Tysoe, J. Electron Spec. Rel. Phenom. 56 (1991) 341.
[48] M.K. Weldon, C.M. Friend, Surf. Sci. 321 (1994) L202.
[49] G. Wu, W.T. Tysoe, Surf. Sci., in press.
[50] L. Wang, W.T. Tysoe, J. Catal. 28 (1991) 320.
[51] B.F. Bartlett, H. Molero, W.T. Tysoe, J. Catal. 167 (1997) 470.
[52] P. Lespade, R. Al-Jishi, M.S. Dresselhaus, Carbon 20 (1982) 427.
[53] D.S. Knight, W.B. White, Mater. Res. 4 (1989) 385.
[54] H.R. Han, L.D. Schmidt, J. Phys. Chem. 75 (1971) 227.
[55] R.C. Weast (Ed.), Handbook of Chemistry and Physics, Chemical Rubber, Cleveland, 1967.
[56] M. Ephritikhine, M.L.H. Green, J. Chem. Soc., Chem. Commun. (1976) 926.
[57] G.J.A. Adams, S.G. Davis, K.A. Ford, M. Ephritikhine, P.F. Todd, M.L.H. Green, J. Mol. Catal. 8 (1980) 15.
[58] G. Wu, W.T. Tysoe, in preparation.
[59] D.T. Laverty, J.J. Rooney, A. Stewart, J. Catal. 5 (1976) 110.
[60] J.E. Deffeyes, A.H. Smith, P.C. Stair, Appl. Surf. Sci. 26 (1986) 517.
[61] J.E. Deffeyes, A.H. Smith, P.C. Stair, Surf. Sci. 163 (1985) 79.
[62] J.W. Robinson (Ed.), Handbook of Spectroscopy, Vol. I, Chemical Rubber, Cleveland, 1974.
[63] H. Molero, W.T. Tysoe, in preparation.